Liquid Crystals
Publication details, including instructions for authors and subscription information:
http://www.informaworld.com/smpp/title~content=t713926090

Why do non-symmetric dimers intercalate? The synthesis and characterisation of the α-(4-benzylidene-substituted-aniline-4'-oxy)-ω-(2-methylbutyl-4'-(4''-phenyl)benzoateoxy)alkanes

Guan-Yeow Yeap[a]; Tiang-Chuan Hng[a]; Sue-Yi Yeap[a]; Ewa Gorecka[b]; Masato M. Ito[c]; Koichi Ueno[c]; Masaki Okamoto[c]; Wan Ahmad Kamil Mahmood[a]; Corrie T. Imrie[d]
[a] Liquid Crystal Research Laboratory, School of Chemical Sciences, Universiti Sains Malaysia, Minden, Penang, Malaysia [b] Department of Chemistry, Warsaw University, Al. Zwirki I Wigury 101, Warsaw, Poland [c] Department of Environmental Engineering for Symbiosis, Faculty of Engineering, Soka University, Hachioji, Tokyo, Japan [d] Chemistry, School of Natural and Computing Sciences, University of Aberdeen, Meston Walk, Aberdeen, UK

Online publication date: 14 December 2009

To cite this Article Yeap, Guan-Yeow , Hng, Tiang-Chuan , Yeap, Sue-Yi , Gorecka, Ewa , Ito, Masato M. , Ueno, Koichi , Okamoto, Masaki , Mahmood, Wan Ahmad Kamil and Imrie, Corrie T.(2009) 'Why do non-symmetric dimers intercalate? The synthesis and characterisation of the α-(4-benzylidene-substituted-aniline-4'-oxy)-ω-(2-methylbutyl-4'-(4''-phenyl)benzoateoxy)alkanes', Liquid Crystals, 36: 12, 1431 — 1441
To link to this Article: DOI: 10.1080/02678290903271504
URL: http://dx.doi.org/10.1080/02678290903271504

Liquid Crystals,
Vol. 36, No. 12, December 2009, 1431–1441

Taylor & Francis
Taylor & Francis Group

Why do non-symmetric dimers intercalate? The synthesis and characterisation of the α-(4-benzylidene-substituted-aniline-4′-oxy)-ω-(2-methylbutyl-4′-(4″-phenyl)benzoateoxy)alkanes

Guan-Yeow Yeap[a]*, Tiang-Chuan Hng[a], Sue-Yi Yeap[a], Ewa Gorecka[b], Masato M. Ito[c], Koichi Ueno[c], Masaki Okamoto[c], Wan Ahmad Kamil Mahmood[a] and Corrie T. Imrie[d]

[a]*Liquid Crystal Research Laboratory, School of Chemical Sciences, Universiti Sains Malaysia, 11800Minden, Penang, Malaysia;* [b]*Department of Chemistry, Warsaw University, Al. Zwirki I Wigury 101, 02-089 Warsaw, Poland;* [c]*Department of Environmental Engineering for Symbiosis, Faculty of Engineering, Soka University, Hachioji, Tokyo 192-8577, Japan;* [d]*Chemistry, School of Natural and Computing Sciences, University of Aberdeen, Meston Walk, Aberdeen AB24 3UE, UK*

(Received 6 July 2009; final version received 24 July 2009)

Ten new non-symmetric liquid crystal dimers belonging to the family of compounds α-(4-benzylidene-substituted-aniline-4′-oxy)-ω-(2-methylbutyl-4′-(4″-phenyl)benzoateoxy)-alkanes have been synthesised and their transitional properties characterised. The dimers contain either a hexamethylene or octamethylene spacer, while the terminal substituents on the 4-benzylideneaniline fragment are H, CH_3, F, Cl and Br. The unsubstituted dimers are not liquid crystalline, while the remaining compounds exhibit enantiotropic nematic behaviour. The trends in the clearing temperatures, according to the chemical nature of the terminal substituent, are largely consistent with those established for conventional low molar mass liquid crystals. Three of the dimers also exhibit an intercalated smectic A phase, specifically the two bromo-substituted dimers and the chloro-substituted dimer containing a hexamethylene spacer. The driving force for the formation of this phase is considered to be, at least in part, the specific anisotropic interaction between the unlike mesogenic units. The absence of smectic behaviour for the isosteric methyl-substituted dimers reveals that steric factors alone cannot stabilise the intercalated smectic A phase.

Keywords: non-symmetric dimers; hexamethylene or octamethylene spacer; enantiotropic nematic behaviour; intercalated smectic A phase

1. Introduction

Liquid crystal oligomers consist of molecules composed of semi-rigid mesogenic units connected via flexible spacers and constitute a class of low molar mass liquid crystals attracting considerable research interest (*1–5*). The simplest oligomers are termed dimers, in which just two mesogenic units are connected by a single spacer and these can be divided into two broad classes, namely, symmetric dimers in which the two mesogenic units are identical and non-symmetric in which they differ. Initial interest in liquid crystal dimers was triggered by their ability to act as model compounds for semi-flexible main chain liquid crystal polymers (*6*), but it soon became apparent, however, that these were fascinating materials in their own right and exhibited quite different behaviour to conventional low molar mass liquid crystals. Examples of recent studies on liquid crystal dimers include investigations of the role of the spacer in determining liquid crystal behaviour (*7–9*), laterally connected dimers (*10*), dimers containing bent-core mesogenic units (*11, 12*), hydrogen-bonded dimers (*13–15*), phase behaviour in bent odd-membered dimers (16) and cholesteryl-containing dimers (*17–24*). In addition to their fundamental interest, dimers also have potential technological applications arising from their flexoelectric behaviour (*25–27*) and light-emitting properties (*28*).

Part of the fascination with liquid crystal dimers can be attributed to the unique smectic behaviour shown by non-symmetric dimers and specifically the discovery of the intercalated smectic phases (*29–31*). An intercalated orthogonal smectic phase composed of non-symmetric dimers may be thought of in terms of two microphase separated domains. Specifically, the differing mesogenic units are mixed to form one domain while the spacers and, if present, the terminal chains constitute another (see Figure 1). A consequence of this molecular arrangement is that a characteristic feature of an intercalated smectic A phase is that the ratio of the smectic periodicity to the estimated all-*trans* molecular length of the dimer is just 0.5. Intercalated smectic phases are generally observed for non-symmetric dimers in which the two differing mesogenic units are thought to exhibit a specific interaction between each other. In turn, such an interaction, which is anisotropic in nature, is often considered to be the driving force for the formation of the phase (*29, 32*). Higher liquid crystal oligomers, such as trimers, consisting of molecules containing three mesogenic units and two spacers (*33*) and tetramers having four mesogenic units and three spacers (*34, 35*), have

*Corresponding author. Email: gyyeap@usm.my or gyyeap_liqcryst_usm@yahoo.com

ISSN 0267-8292 print/ISSN 1366-5855 online

DOI: 10.1080/02678290903271504
http://www.informaworld.com

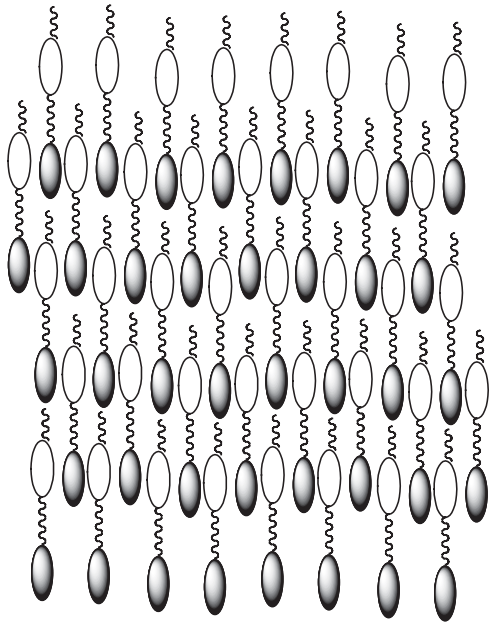

Figure 1. A sketch of the local molecular organisation within an intercalated smectic A phase composed of non-symmetric dimers.

been prepared containing different mesogenic units (*36–39*) and also show intercalated smectic phases. The driving force for the formation of these phases again is most often attributed to a specific interaction between the unlike mesogenic groups.

It is important to note, however, that intercalated smectic phases have also been observed for a small number of symmetric dimers (*7*, *40–44*). It is not clear what drives the formation of the intercalated arrangement in these cases, although it has been suggested that specific dipolar interactions between the mesogenic units may play an important role (*1*).

Although a large number of non-symmetric dimers are now known to exhibit intercalated smectic phases and the molecular organisation sketched in Figure 1 is widely accepted, there remain a number of features regarding these phases that are not well understood. It is not clear, for example, how space can be filled efficiently for dimers in which there is a significant mismatch in the lengths of the spacer and terminal chain (*30*) or why excluded volume or space filling constraints do not drive the formation of intercalated phases (*31, 45*). In order to understand better the factors influencing the formation and stability of intercalated smectic phases, we report here the transitional properties of new non-symmetric liquid crystal dimers, the structures of which are shown in Figure 2. We refer to these compounds using the acronym **MB-*n*-X**, in which **MB** denotes the 2-methyl butyl terminal chain, ***n*** the number of methylene units in the flexible alkyl spacer and **X** the chemical nature of

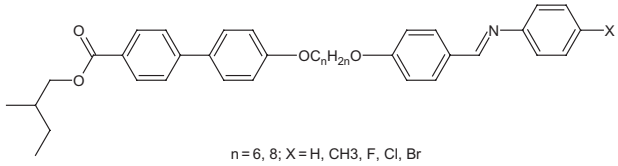

Figure 2. Structures of the non-symmetric liquid crystal dimers, **MB-*n*-X**.

the other terminal substituent. By systematically varying the spacer lengths and terminal substituents in these dimers, our aim, in particular, is to probe the relationships between the steric and electronic effects and the formation of intercalated smectic phases. A branched terminal chain has been selected because, to our knowledge, the majority of dimers known to exhibit intercalated smectic phases contain a linear terminal chain and this will allow us to investigate space filling constraints on the stability of the phases. We should also note that in this particular study we have not included the nitrile group because this has been widely studied in this context (*1–5*) and our focus here is rather on more unusual groups in terms of the formation of intercalated smectic phases.

2. Experimental

The starting materials, including the 2-methyl-1-butanol, were purchased from either Acros Organics (Belgium) or Sigma Aldrich (USA), except for the 4-(4-hydroxyphenyl)benzoic acid, which was obtained from Tokyo Chemical Industry (Japan). All were used as received.

2.1 Synthesis

The syntheses of the intermediate compounds **1**, **2a–e** and **3a–j** and the non-symmetric liquid crystal dimers, **MB-*n*-X**, were undertaken using the synthetic routes shown in Scheme 1. The codes used to refer to intermediate compounds **2** and **3** are listed in Tables 1 and 2, respectively. All of the intermediates and final products were characterised using infrared (IR) and ^{1}H-nuclear magnetic resonance (NMR) spectroscopy and their spectra were found to be consistent with the proposed structures. In addition, satisfactory elemental analyses were obtained for all compounds. Representative characterisation data are provided for one representative member of each set of new materials.

*2.1.1 Synthesis of compound **1***

4-(4-hydroxyphenyl)benzoic acid (1.50 g, 7.0 mmole) was added to 2-methyl-1-butanol (25 ml), which

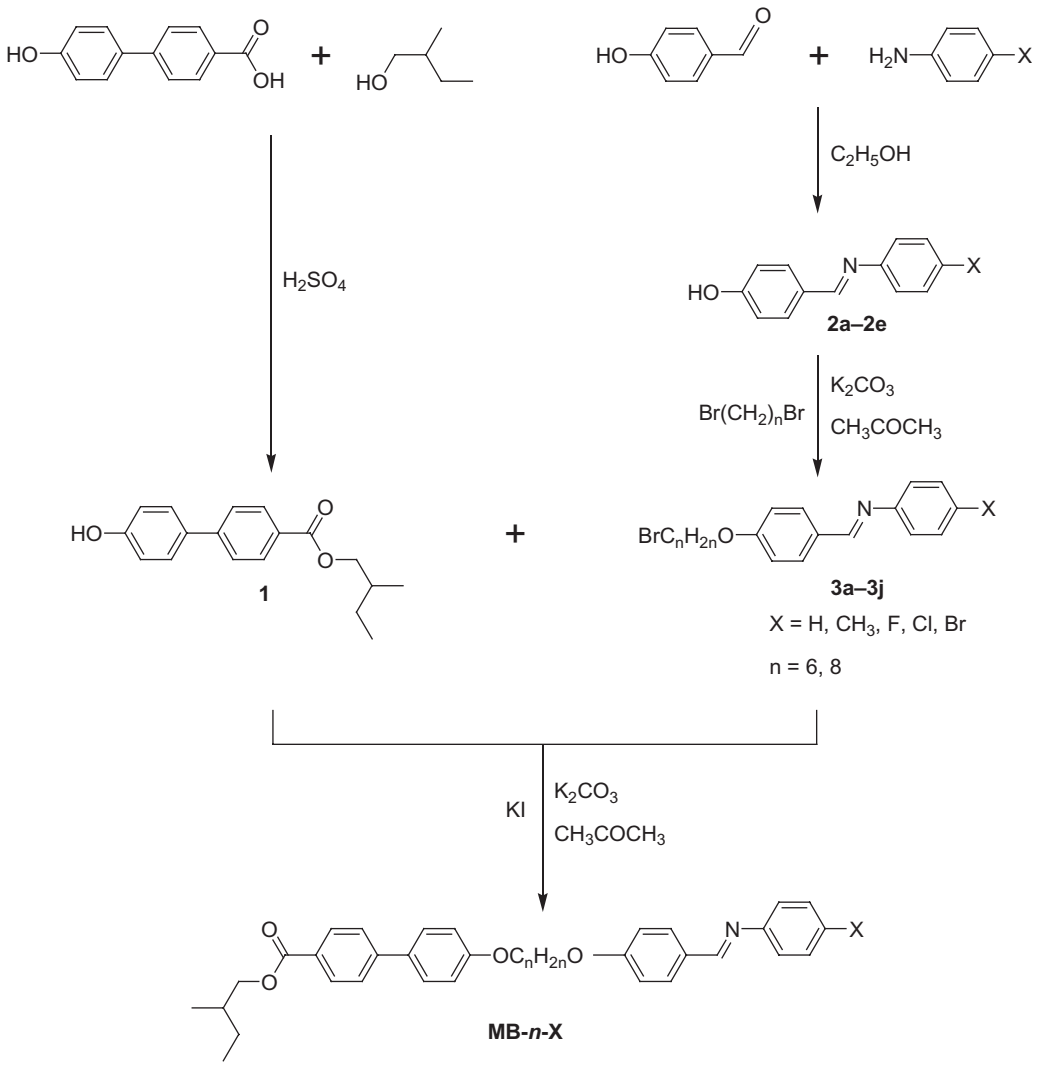

Scheme 1. Synthetic route for the preparation of the liquid crystal dimers **MB-*n*-X**.

Table 1. Codes used to refer to compounds **2a–e** in Scheme 1.

Intermediate	Terminal substituent, X
2a	H
2b	CH_3
2c	F
2d	Cl
2e	Br

Table 2. Codes used to refer to compounds **3a–j** as shown in Scheme 1.

Intermediate	Terminal substituent, X	Spacer ($-C_nH_{2n}-$)
3a	H	C_6H_{12}
3b	CH_3	C_6H_{12}
3c	F	C_6H_{12}
3d	Cl	C_6H_{12}
3e	Br	C_6H_{12}
3f	H	C_8H_{16}
3g	CH_3	C_8H_{16}
3h	F	C_8H_{16}
3i	Cl	C_8H_{16}
3j	Br	C_8H_{16}

served both as a reactant and the reaction solvent. As the temperature was increased, a catalytic amount of concentrated H_2SO_4 was added dropwise and the reaction mixture heated at 90°C for 24 h. The mixture was cooled to room temperature and extracted using an aqueous solution of sodium bicarbonate. This aqueous layer was subsequently washed three times with ether. The combined ether solution was left to allow the solvent to evaporate and the crude product was recrystallised from chloroform. Yield 70%. Elemental analysis: found, C 76.04, H 7.11; calculated ($C_{18}H_{20}O_3$), C 76.03, H 7.09. IR (KBr) ν cm^{-1}, 3409

(OH), 2967–2878 (C–H alkyl), 1683 (C=O ester). ^{1}H-NMR ($CDCl_3$) δ ppm^{-1}, 0.99 (t, 3H, CH_3), 1.06 (d, 3H, CH_3), 1.57 (m, 2H, CH_2), 1.90 (m, 1H, CH), 4.16–4.28 (2dd, 2H, $COOCH_2$), 6.98 (d, 2H, Ar), 7.54 (d, 2H, Ar), 7.65 (d, 2H, Ar), 8.10 (d, 2H, Ar).

2.1.2 *Synthesis of compounds **2a**–**2e***

4-Hydroxybenzaldehyde (1.21 g, 9.9 mmole) was dissolved in absolute ethanol (40 ml). An ethanolic solution of the appropriately substituted aniline (9.9 mmole) was added dropwise and the mixture heated at 70°C for 22 h. The resulting solution was left to evaporate to dryness at room temperature to give a brown precipitate. The crude product was recrystallised twice using chloroform to yield the desired Schiff base intermediate.

2a Yield 80%. Elemental analysis: found, C 79.18, H 5.63, N 7.10; calculated ($C_{13}H_{11}NO$), C 79.16, H 5.62, N 7.10. IR (KBr) ν cm^{-1}, 3413 (OH), 1611–1603 (C=N). ^{1}H-NMR ($CDCl_3$) δ ppm^{-1}, 5.25 (s, 1H, OH), 6.94 (d, 2H, Ar), 7.22 (m, 3H, Ar), 7.41 (t, 2H, Ar), 7.82 (d, 2H, Ar), 8.40 (s, 1H, CH=N).

2.1.3 *Synthesis of **3a***

2a (0.28 g, 1.4 mmole) was mixed with 1,6-dibromohexane (2.05 g, 8.4 mmole) and dissolved in acetone (50 ml). Potassium carbonate anhydrous (0.77 g, 5.6 mmole) was added to the stirred solution and the mixture was refluxed for 18 h. The reaction mixture was allowed to cool and left to allow the solvent to evaporate at room temperature. Water (50 ml) was added and the resulting precipitate filtered and dried. The crude product was recrystallised from chloroform. Yield 67%. Elemental analysis: found, C 63.35, H 6.17, N 3.89; calculated ($C_{19}H_{22}BrNO$), C 63.34, H 6.15, N 3.89. IR (KBr) ν cm^{-1}, 2938–2862 (C–H alkyl), 1620–1606 (C=N), 1252 (O–CH_2). ^{1}H-NMR ($CDCl_3$) δ ppm^{-1}, 1.54–1.93 (m, 8H, CH_2), 3.46 (t, 2H, CH_2Br), 4.05 (t, 2H, OCH_2), 7.00 (dd, 2H, Ar), 7.23 (m, 3H, Ar), 7.41 (t, 2H, Ar), 7.87 (d, 2H, Ar), 8.40 (s, 1H, CH=N).

2.1.4 *Synthesis of **MB-6-H***

1 (0.11 g, 0.4 mmole) and **3a** (0.14 g, 0.4 mmole) were dissolved in stirred acetone (40 ml). Anhydrous potassium carbonate (0.17 g, 1.2 mmole) was added to the solution, together with a catalytic amount of potassium iodide as the temperature was increased. The reaction mixture was heated at reflux for 12 h. The mixture was allowed to cool and left to allow the solvent to evaporate at room temperature. Water (50 ml) was added and the resulting precipitate filtered, washed using acetone and recrystallised from chloroform. Yield 34%. Elemental analysis: found, C 78.85, H 7.36, N 2.49; calculated ($C_{37}H_{41}NO_4$), C 78.83, H 7.33, N 2.48. IR (KBr) ν cm^{-1}, 2939–2874 (C–H alkyl), 1715 (C=O ester), 1621–1606 (C=N), 1251 (O–CH_2). ^{1}H-NMR ($CDCl_3$) δ ppm^{-1}, 0.99 (t, 3H, CH_3), 1.06 (d, 3H, CH_3), 1.34 (m, 1H, CH), 1.56–1.95 (m, 10H, CH_2), 4.08 (m, 4H, OCH_2), 4.15–4.26 (2dd, 2H, $COOCH_2$), 6.99 (2d, 4H, Ar), 7.23 (m, 3H, Ar), 7.41 (t, 2H, Ar), 7.58 (d, 2H, Ar), 7.66 (d, 2H, Ar), 7.85 (d, 2H, Ar), 8.12 (d, 2H, Ar), 8.41 (s, 1H, CH=N).

2.2 *Characterisation*

The Fourier transform infrared (FTIR) spectra for all of the intermediate and target compounds were obtained using a Perkin Elmer 2000 FTIR spectrophotometer. The samples were mixed with KBr and the spectra recorded in the range 4000–400 cm^{-1}. ^{1}H-NMR spectra were obtained using a Bruker 400 MHz Ultrashield^{TM} spectrometer. The samples were dissolved in $CDCl_3$ with tetramethylsilane (TMS) as the internal standard. For the intermediates **2a**–**2e**, the spectra were collected at 50°C because the solubility of these compounds in $CDCl_3$ at room temperature was insufficient. CHN microanalyses were conducted using a Perkin Elmer 2400 LS Series CHNS/O Analyser. The optical textures of the phases shown by the dimers were observed using a Carl Zeiss Axioskop 40 polarising microscope equipped with a Linkam TMS94 temperature controller and an LTS350 hot-stage. The microphotographs of the mesophase textures were taken for samples during heating or cooling at 3°C min^{-1}. The transition temperatures and associated enthalpy changes were measured using a Seiko DSC120 Model 5500 differential scanning calorimeter. All differential scanning calorimetry (DSC) traces were recorded with heating and cooling rates of 2°C min^{-1}. The powder X-ray diffraction measurements were performed using a wide-angle Bruker D8 diffractometer (CuK_α line) and powder samples contained in the capillaries.

3. Results and discussion

The transition temperatures, associated enthalpy changes and nematic–isotropic entropy changes of the non-symmetric dimers **MB-*n*-X** are listed in Table 3. The DSC heating–cooling traces for a representative compound **MB-6-F** are given in Figure 3. All the dimers, except those without a terminal substituent, i.e. **MB-6-H** and **MB-8-H**, exhibit enantiotropic liquid-crystalline behaviour. The methyl-substituted dimers, **MB-6-CH$_3$** and **MB-8-CH$_3$**, show exclusively

Table 3. The transitional properties of the **MB-*n*-X** dimers.

MB-*n*-X	T_{Cr}/°C	T_{SmA_cN}/°C	T_{NI}/°C	ΔH_{Cr}/kJ mol^{-1}	ΔH_{SmAN}/kJ mol^{-1}	ΔH_{NI}/kJ mol^{-1}	$\Delta S_{NI}/R$
MB-6-H	121.1	–	(118.5)	59.8	–	–[a]	–
MB-6-CH$_3$	113.6	–	162.3	27.2	–	4.0	1.11
MB-6-F	119.2	–	150.0	36.2	–	3.4	0.98
MB-6-Cl	109.8	108.8	165.3	30.2	0[b]	3.7	1.01
MB-6-Br	109.0	116.0	165.9	30.8	0[b]	4.0	1.08
MB-8-H	101.6	–	(99.8)[a]	59.2	–	–	–
MB-8-CH$_3$	98.4	–	139.7	36.3	–	4.8	1.38
MB-8-F	116.3	–	126.8	37.1	–	3.4	1.03
MB-8-Cl	100.5	–	134.0	29.7	–	3.2	0.98
MB-8-Br	95.1	140.0	152.6	23.2	1.9	4.0	1.13

[a]Crystallisation precluded measurement of the enthalpy change.
[b]Transition not detected by DSC.
( )Indicates monotropic transitions.

nematic behaviour. The nematic phases of both dimers were identified on the basis of the observation of characteristic marble textures on heating, while on cooling from the isotropic phase, the nematic phase of **MB-8-CH$_3$** showed a thread-like texture. The fluoro-substituted dimers **MB-6-F** and **MB-8-F** are also solely nematogenic. The nematic phases were assigned from their schlieren optical textures, containing both types of point singularity, which flashed when subjected to mechanical stress. The chloro-substituted dimer containing an octamethylene spacer, **MB-8-Cl**, also shows only a nematic phase, which was assigned on the basis of the observation of a characteristic schlieren texture; a representative texture is shown in Figure 4. By comparison, on cooling the nematic phase of the corresponding dimer containing a hexamethylene spacer, **MB-6-Cl**, the schlieren texture changed to give a focal-conic fan texture characteristic of a smectic A phase. This transition was not detected using DSC and the monotropic nature of the phase precluded its study using X-ray diffraction. Specifically, the smectic A phase

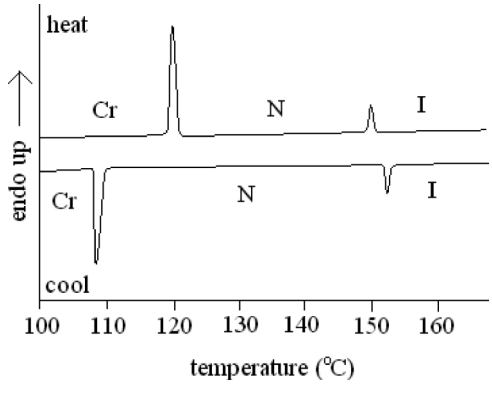

Figure 3. DSC trace for compound **MB-6-F** on heating and cooling cycles at the rate of ±2°C min^{-1}.

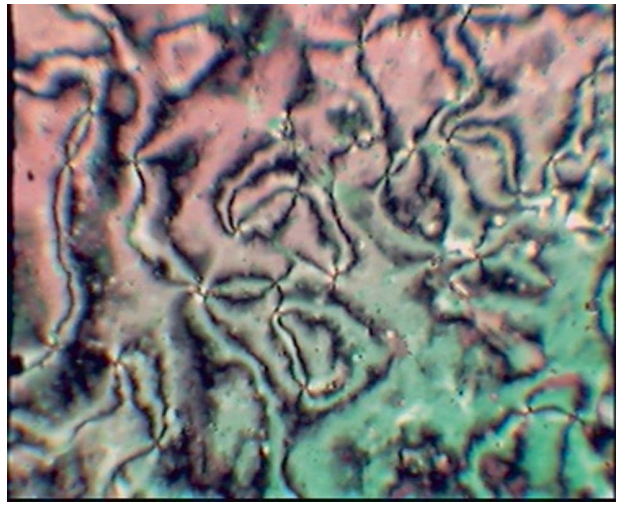

Figure 4. The schlieren texture for the nematic phase of compound **MB-8-Cl** at 131.4°C.

crystallised on the time-scale of the X-ray diffraction experiment. Both bromo-substituted dimers, **MB-6-Br** and **MB-8-Br**, show enantiotropic smectic A and nematic phases assigned from the characteristic schlieren nematic texture, which changed on cooling to give focal-conic fan textures in coexistence with homeotropic domains; a representative focal conic fan texture observed for **MB-6-Br** is shown in Figure 5. It is interesting to note that the focal-conic fan texture of the smectic phase also contains polygonal defects. The smectic A–nematic transition for **MB-6-Br** was not seen by DSC, whereas that shown by **MB-8-Br** was detected and we will return to a discussion of this later. The two unsubstituted dimers, **MB-6-H** and **MB-8-H**, melted directly into the isotropic phase, but on cooling the isotropic phase and prior to crystallisation, a schlieren texture was observed characteristic of a

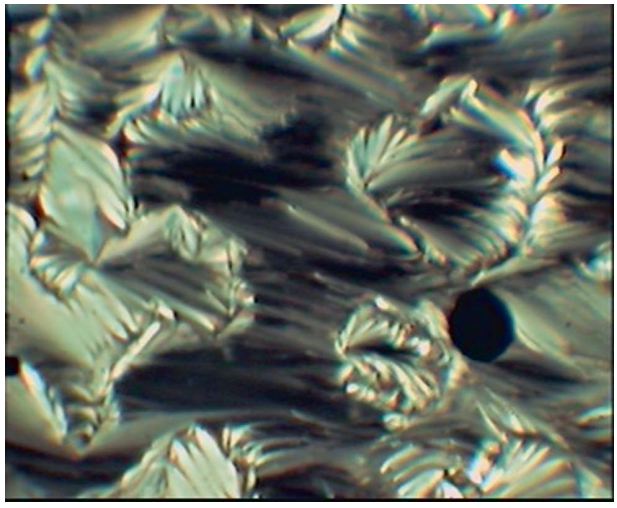

Figure 5. The focal-conic fan texture, containing polygonal defects, for the smectic A phase of compound **MB-6-Br** at 114.5°C.

nematic phase. Rapid crystallisation of this monotropic phase prevented the evaluation of the nematic–isotropic enthalpy change using DSC.

If we first consider the melting points of these dimers, then for the hexamethylene spacer, the melting point decreases according to the terminal substituent in the order:

$$H > F > CH_3 > Cl \approx Br,$$

while for the octamethylene spacer, the order is:

$$F > H > Cl > CH_3 > Br.$$

Thus, there appears to be no regular trend across the two series in how the terminal substituent affects the melting point, but it should be noted that for every corresponding pair of dimers the one containing the hexamethylene spacer has the higher melting point. This is characteristic behaviour for a homologous series of liquid-crystal dimers for which the melting points of the even members tend to decrease on increasing the spacer length (*1–4*).

The efficiency of the terminal substituent in enhancing the nematic–isotropic transition temperature for dimers with a hexamethylene spacer is:

$$Br \approx Cl > CH_3 > F > H,$$

while for the octamethylene spacer the order is:

$$Br > CH_3 > Cl > F > H.$$

These trends are broadly consistent with those observed for conventional low molar mass liquid crystals possessing just a single mesogenic unit (*46*) and most commonly rationalised in terms of the size of the substituent and its ability to interact with the mesogenic unit. Figure 6 shows the dependence of the nematic–isotropic transition temperature on the van der Waals radius of the terminal substituent, X, for the two sets of dimers. For each spacer length, the transition temperatures, at least to a first approximation, are more or less linearly dependent on the size of the terminal substituent with the marked exception of the **MB-*n*-H** homologues for which the T_{NI} are considerably lower than would be expected. It is surprising, however, that the addition of a single and relatively small substituent should have such a large relative effect on the nematic–isotropic transition temperature, T_{NI}, when compared to the T_{NI} of the unsubstituted dimers **MB-6-H** and **MB-8-H**. The percentage increase in the molecular length on exchanging a terminal H atom for any one of these substituents is considerably smaller than the associated percentage increase in the clearing temperature and would appear far too small to account for the change in T_{NI}.

Similar observations have been made for other dimer series and it has been suggested that the dramatic increase in T_{NI} may result from a change in shape on substituting the mesogenic unit rather than from any significant enhancement of the shape anisotropy (*30*). Similar to the case of the melting points, for each pair of corresponding dimers the members with a hexamethylene spacer show the higher T_{NI}. Indeed, the commonly observed trend within a homologous series of dimers is that the clearing temperature of the even members decreases on increasing spacer length (*1–4*). A difference in shape on changing the terminal substituent may also be inferred from the spread in T_{NI}, which is smaller for the dimers containing the hexamethylene spacer. Thus, the terminal substituent has a larger relative effect on T_{NI} for the dimers

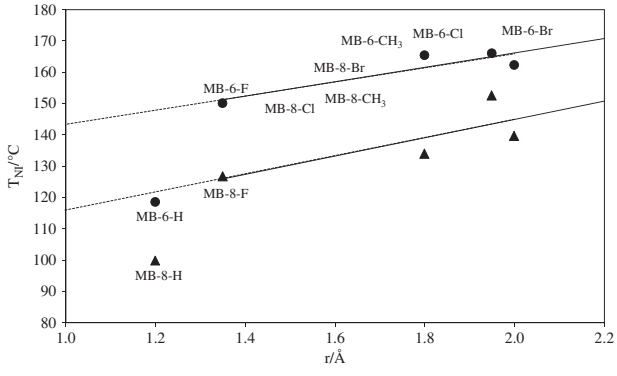

Figure 6. Dependence of the nematic–isotropic transition temperature on the van der Waals radius of substituent X for the **MB-*n*-X** dimers.

containing an octamethylene spacer because the two mesogenic units are less well orientationally coupled and, hence, the substituent has a greater relative effect on the shape anisotropy of the unit to which it is attached.

The entropy changes associated with the nematic–isotropic transition of these dimers expressed as the dimensionless quantity, $\Delta S_{NI}/R$, fall in the range 0.98–1.38, which is somewhat lower than normally observed for liquid-crystal dimers containing terminal linear alkyl chains or small terminal substituents (*47–51*). The $\Delta S_{NI}/R$ values of the dimers with an octamethylene spacer are generally higher as compared to the hexamethylene counterparts with the same substituents except for **MB-8-Cl** (see Table 3) and this is archetypal behaviour for a series of dimers for which the nematic–isotropic entropy change increases for even members on increasing the spacer length. The values of $\Delta S_{NI}/R$ for **MB-6-Cl** and **MB-8-Cl** are the same within experimental error. The low values of $\Delta S_{NI}/R$ exhibited by the **MB-*n*-X** dimers may be attributed to the branched chain, which increases molecular biaxiality resulting from the decreased length-to-breadth ratio relative to unbranched analogues. Similar reductions have been observed for other dimers containing branched terminal chains (*52*) and also for dimers in which the biaxiality of the mesogenic groups has been increased (*53–55*). We now turn our attention to the smectic behaviour of these dimers. As we have seen, three of the ten dimers exhibit a smectic A phase, namely, those possessing a hexamethylene spacer and either a chlorine atom, **MB-6-Cl,** or bromine atom, **MB-6-Br,** and that with an octamethylene spacer and a bromine atom, **MB-8-Br**. In order to confirm the smectic A phase assignments and to determine the molecular arrangement within the phase, X-ray diffraction studies were performed. Figure 7 shows the intensity profile of the X-ray diffraction powder pattern of the smectic A phase shown by **MB-6-Br**. A weak, sharp reflection is evident in the low-angle region arising from the layered structure of the smectic A phase, while in the wide-angle region a broad peak centred at 4.5 Å is present, characteristic of the liquid-like arrangement of the molecules within the layers. The layer spacing in the smectic phase is 18.3 Å, which is approximately half the estimated all-*trans* molecular length of 37.0 Å for **MB-6-Br**. This indicates that the phase may be assigned as an intercalated smectic A phase, SmA_c, in which the molecules form an interleaved structure with differing parts of the molecules overlapping (see Figure 8). It is important to note that the molecular arrangement shown in Figure 8 is ferroelectric, but these molecular groupings will be randomly arranged at the macroscopic level such that ferroelectric properties are not expected to be observed. The relatively weak

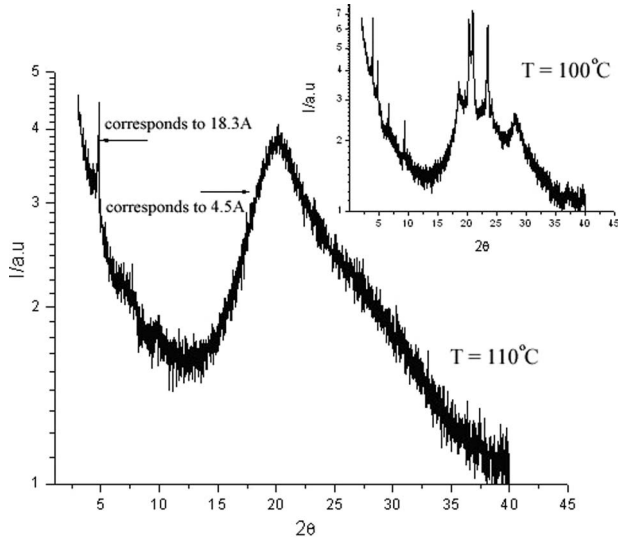

Figure 7. The intensity versus 2θ profile for the X-ray diffraction powder pattern of compound **MB-6-Br** in the intercalated SmA_c phase at 110°C. The inset shows the intensity versus 2θ profile in the Cr phase at 100°C.

intensity of the signal in the X-ray pattern shown in Figure 7 at low angles indicates that the electron density modulation depth along the layer normal in this system is low, which arises from the intercalation of the molecules. The observation of only the first-order layer reflection in the intensity profile indicates that the density profile along the layer normal is close to sinusoidal. The asymmetry at $2\theta = 20°$ in the X-ray diffraction profile is presumably due to overlapping of the signals arising from the sample and from the amorphous glass capillary holding the sample. The inset in Figure 7 shows the intensity profile of the X-ray diffraction powder pattern of the crystal phase and a number of reflections can be observed in both the low- and wide-angle regions, indicative of a three-dimensional arrangement. A similar X-ray diffraction pattern was obtained for the smectic A phase exhibited by **MB-8-Br** and the layer periodicity was measured as 18.8 Å. Again this indicates an intercalated arrangement of the molecules within the smectic A phase. The monotropic nature of the smectic A phase exhibited by **MB-6-Cl** precluded its characterisation using X-ray diffraction.

As we have noted already, the driving force for the formation of the intercalated smectic A phase is most often attributed, at least in part, to a specific, favourable interaction, which is anisotropic, between the unlike mesogenic groups. This interaction was suggested to be an electrostatic quadrupolar interaction between groups having quadrupole moments of opposite signs (*56*). In addition, the mixing of the unlike mesogenic units required to maximise the extent of this interaction is entropically more favourable than

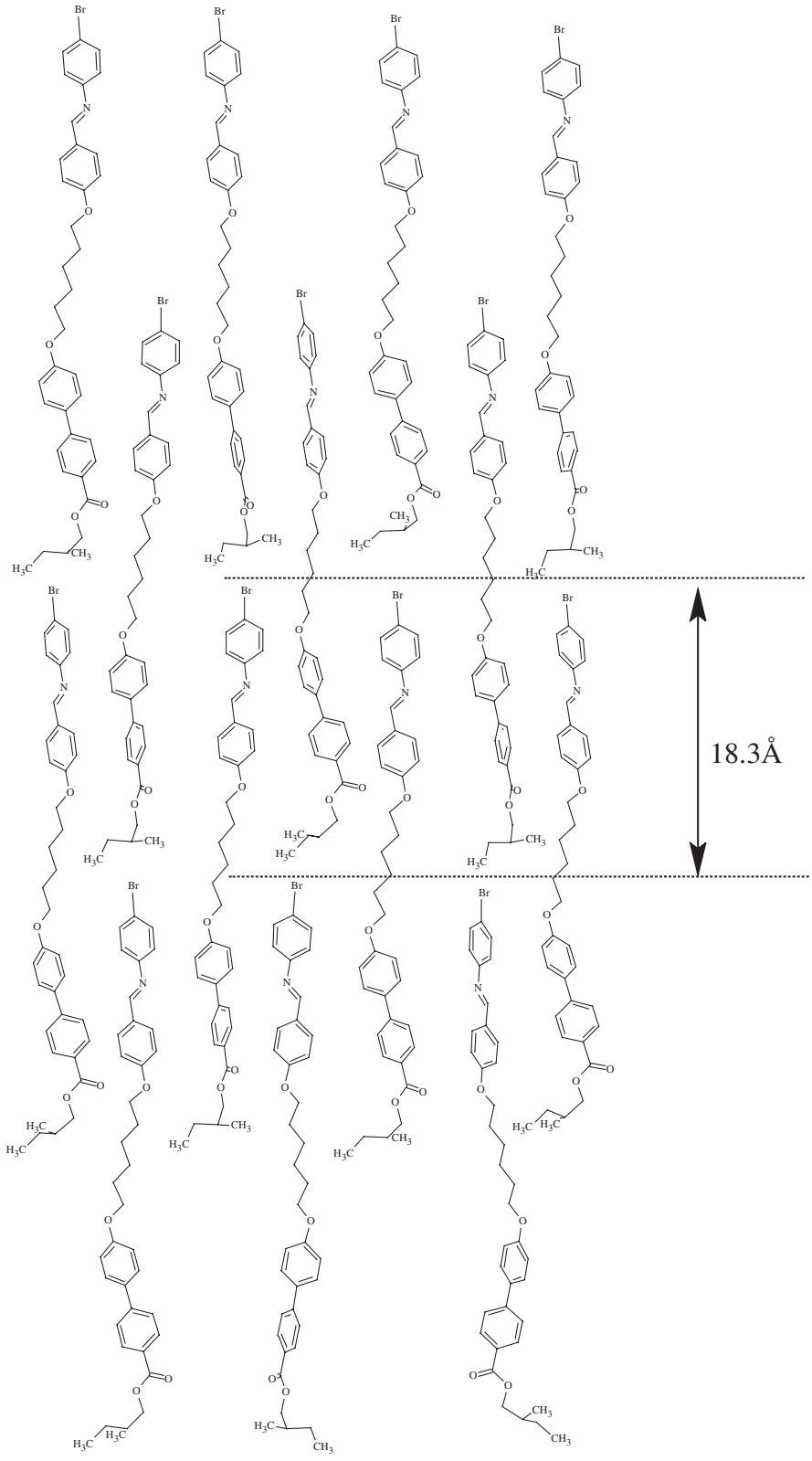

Figure 8. A sketch of the molecular organisation within the intercalated smectic A phase shown by **MB-6-Br**. The layer periodicity of 18.3Å is indicated.

allowing the dimers to microphase separate into domains consisting of like mesogenic units, spacers and terminal chains. What is often overlooked, however, is that this interaction alone cannot explain the formation of the phase, because these enthalpic and entropic contributions would be identical in a conventional monolayer phase. It would appear, therefore, that the entropic gain in mixing the terminal chain and spacer must also be important and in designing these dimers we chose a terminal chain that could be accommodated in the space between the layers which, in an intercalated arrangement, is determined largely by the length of the spacer (see Figure 8).

For the dimers containing the hexamethylene spacer, the bromo-substituted dimer, **MB-6-Br**, has a higher smectic A–nematic transition temperature, T_{SmAN}, than for the chloro-substituted dimer, **MB-6-Cl**. This may indicate an enhancement in the strength of the interaction between the unlike cores on replacing the chlorine atom by a bromine. It is also tempting to suggest that the larger bromine substituent fills space more effectively in the intercalated structure. If the trend in T_{SmAN} was to continue to the fluoro-substituted dimer, **MB-6-F**, then the smectic phase would be strongly monotropic and experimentally crystallisation precluded the possibility of observing smectic behaviour. Indeed, rapid cooling of the nematic phase shown by **MB-6-F** did not lower the crystallisation temperature significantly.

For the octamethylene-spacer homologues only the bromo-substituted dimer, **MB-8-Br**, showed smectic behaviour revealing that the increase in T_{SmAN} on passing from a chloro, **MB-8-Cl**, to a bromo group, **MB-8-Br**, is very much larger than that observed for the corresponding hexamethylene-spacer dimers. It is far from clear why this should be the case, although it is interesting to note that there is also a much larger difference in T_{NI} between **MB-8-Cl** and **MB-8-Br** than for **MB-6-Cl** and **MB-6-Br**. The absence of smectic A behaviour for the fluoro-substituted dimer, **MB-8-F**, may again be attributed to the higher melting point of the compound. We should note that our attempts to supercool the nematic phases shown by **MB-8-F** and **MB-8-Cl** in order to reveal smectic behaviour did not, in fact, significantly reduce the crystallisation temperature.

The entropy change associated with the smectic A–nematic transition, $\Delta S_{SmAN}/R$, is essentially zero for **MB-6-Cl** and **MB-6-Br** but equal to 0.56 for **MB-8-Br**. This may be rationalised in terms of the McMillan theory (*57*), which predicts that $\Delta S_{SmAN}/R$ increases as the nematic temperature range decreases (*4*). This can be measured in terms of the McMillan parameter, T_{SmAN}/T_{NI}, which for **MB-6-Cl** is 0.871 and for **MB-6-Br** is 0.886, while for **MB-8-Br** is 0.970. Thus, as the McMillan parameter increases, so does $\Delta S_{SmAN}/R$. Similar behaviour has been observed for other dimers (*41*).

The question does arise, however, whether those dimers that do not exhibit smectic behaviour have a localised intercalated arrangement of the molecules in the nematic phase. The small-angle peak in the X-ray diffraction pattern of the nematic phase exhibited by **MB-6-F** is extremely weak, indicating that the electron density is highly uniform along the molecular long axis, and corresponds to a repeat distance of 16.5 Å among molecules. This is approximately half the molecular length of 35.8 Å, implying a localised intercalated arrangement of molecules. An essentially identical X-ray pattern was obtained for the nematic phase of **MB-8-F**, for which the repeat distance was 18.4 Å. Again this is approximately half the actual molecular length implying an intercalation occurred, at the local level, among the nematogenic dimers.

We turn our attention now to the methyl-substituted homologues, **MB-6-CH$_3$** and **MB-8-CH$_3$**. The effective molecular length in the nematic phase of **MB-6-CH$_3$** measured using X-ray diffraction is 33.5 Å, which is similar to the estimated molecular length of 35.1 Å. The X-ray diffraction pattern obtained for the nematic phase of **MB-8-CH$_3$** contained two reflections in the small-angle region, corresponding to repeat distances of 38 and 19 Å. The estimated molecular length of **MB-8-CH$_3$** is 38.1 Å. One interpretation of the X-ray pattern involves a frustrated localised arrangement of the molecules giving rise to two competing periodicities approximately equal to the molecular length and half the molecular length. A more plausible explanation, however, involves smectic fluctuations or cybotactic clusters within the nematic phase and the small-angle reflections correspond to the first and second order reflections from these.

We have seen, therefore, that the halogen substituted dimers have a tendency to adopt intercalated arrangements, whereas the methyl-substituted dimers do not. This strongly reinforces the view that the specific interaction between the unlike cores is central to the formation of the intercalated arrangement. Instead, if steric considerations provided the driving force, then it would be expected that the essentially isosteric bromo- and methyl-substituted compounds would behave in a more similar fashion, which indeed they do in terms of the clearing temperature.

4. Conclusions

This systematic study of structure–property relationships in liquid crystal dimers, with a particular focus on understanding the links between molecular structures and the observation of intercalated smectic

phases, provides further evidence that space-filling constraints do not play a major role in driving the formation of these phases. Indeed, a prerequisite for the observation of an intercalated smectic phase in non-symmetric dimers appears to be the existence of a specific interaction between the unlike mesogenic units.

Acknowledgements

The corresponding author (G.-Y. Yeap) wishes to thank the Malaysian government, and in particular the Higher Education Ministry and the Ministry of Science, Technology and Innovation (MOSTI), for financial support through the provision of the Fundamental Research Grant Scheme (FRGS Grant No. 203/PKIMIA/671025), as well as eScience (Grant No. 305/PKIMIA/613328). The indirect contribution from staff in the Research and Creativity Management Office (RCMO) of the Universiti Sains Malaysia has also been essential to ensure the success of this project.

References

(1) Imrie, C.T.; Luckhurst, G.R. In *Handbook of Liquid Crystals*; Demus, D., Goodby, J.W., Gray, G.W., Spiess, H.W. and Vill, V., Eds.; Wiley-VCH: Weinheim, 1998; pp 801–803, Vol 2B.
(2) Imrie, C.T. *Struct. Bond.* **1999**, *95*, 149–192.
(3) Imrie, C.T.; Henderson, P.A. *Curr. Opin. Colloid Interface Sci.* **2002**, *7*, 298–311.
(4) Imrie, C.T.; Henderson, P.A. *Chem. Soc. Rev.* **2007**, *36*, 2096–2124.
(5) Imrie, C.T.; Henderson, P.A.; Yeap, G.Y. *Liq. Cryst*. **2009**, *36*, 755–777.
(6) Luckhurst, G.R. *Macromol. Symp.* **1995**, *96*, 1–26.
(7) Pal, S.K.; Raghunathan, W.A.; Kumar, S. *Liq. Cryst.* **2007**, *34*, 135–141.
(8) Yoshizawa, A.; Kawaguchi, T. *Liq. Cryst.* **2007**, *34*, 177–181.
(9) Centore, R. *Liq. Cryst.* **2007**, *34*, 729–736.
(10) Yoshizawa, A.; Iwamochi, H.; Segawa, S.; Sato, M. *Liq. Cryst*. **2007**, *34*, 1039–1044.
(11) Achten, R.; Koudijs, A.; Giesbers, M.; Marcelis, A.T.M.; Sudhölter, E.J.R.; Schroeder, M.W.; Weissflog, W. *Liq. Cryst.* **2007**, *34*, 59–64.
(12) Umadevi, S.; Sadashiva, B.K. *Liq. Cryst*. **2007**, *34*, 673–681.
(13) Toh, C.L.; Xu, J.; Lu, X.; He, C. *Liq. Cryst*. **2008**, *35*, 241–251.
(14) Bai, B.; Wang, H.; Zhang, P.; Qu, S.; Li, F.; Yu, Z.; Long, B.; Li, M. *Liq. Cryst*. **2008**, *35*, 793–798.
(15) Wang, H.; Shao, R.; Zhu, C.; Bai, B.; Gong, C.; Zhang, P.; Li, F.; Li, M.; Clark, N.A. *Liq. Cryst*. **2008**, *35*, 967–974.
(16) Bialecka-Florjanczyk, E.; Sledzinska, I.; Gorecka, E.; Przedmojski, J. *Liq. Cryst*. **2008**, *35*, 401–406.
(17) Zhang, C.; Jin, L.; Yin, B.; Jamil, M. *Liq. Cryst.* **2008**, *35*, 39–44.
(18) Wu, C.C. *Liq. Cryst*. **2007**, *34*, 283–288.
(19) Yelamaggad, C.V.; Shanker, G. *Liq. Cryst.* **2007**, *34*, 799–809.
(20) Yelamaggad, C.V.; Shanker, G. *Liq. Cryst*. **2007**, *34*, 1045–1057.
(21) Sharma, R.K.; Gupta, V.K.; Mathews, M.; Yelamaggad, C.V. *Liq. Cryst*. **2008**, *35*, 1161–1167.
(22) Yelamaggad, C.V.; Shashikala, I.S.; Hiremath, U.S.; Rao, D.S.S.; Prasad, S.K. *Liq. Cryst*. **2007**, *34*, 153–167.
(23) Pandey, A.S.; Dhar, R.; Pandey, M.B.; Achalkumar, A.S.; Yelamaggad, C.V. *Liq. Cryst.* **2009**, *36*, 13–19.
(24) Apreutesei, D.; Mehl, G.H.; Scutaru, D. *Liq. Cryst*. **2007**, *34*, 819–831.
(25) Ferrarini, A.; Greco, C.; Luckhurst, G.R. *J. Mater. Chem*. **2007**, *17*, 1039–1042.
(26) Aziz, N.; Kelly, S.M.; Duffy, W.; Goulding, M. *Liq. Cryst*. **2008**, *35*, 1279–1292.
(27) Morris, S.M.; Clarke, M.J.; Blatch, A.E.; Coles, H.J. *Phys. Rev. E.* **2007**, *75*, 041701.
(28) Srivastava, R.M.; Filho, R.A.W.N.; Schneider, R.; Vieira, A.A.; Gallardo, H. *Liq. Cryst.* **2008**, *35*, 737–742.
(29) Hogan, J.L.; Imrie, C.T.; Luckhurst, G.R. *Liq. Cryst.* **1988**, *3*, 645–650.
(30) Attard, G.S.; Date, R.W.; Imrie, C.T.; Luckhurst, G.R.; Roskilly, S.J.; Seddon, J.M.; Taylor, L. *Liq. Cryst.* **1994**, *16*, 529–581.
(31) Imrie, C.T. *Liq. Cryst.* **2006**, *33*, 1449–1454.
(32) Attard, G.S.; Garnett, S.; Hickman, C.G.; Imrie, C.T.; Taylor, L. *Liq. Cryst.* **1990**, *7*, 495–508.
(33) Imrie, C.T.; Luckhurst, G.R. *J. Mater. Chem*. **1998**, *8*, 1339–1343.
(34) Henderson, P.A.; Imrie, C.T. *Liq. Cryst.* **2005**, *32*, 1531–1541.
(35) Henderson, P.A.; Imrie, C.T. *Macromolecules* **2005**, *38*, 3307–3311.
(36) Imrie, C.T.; Henderson, P.A.; Seddon, J.M. *J. Mater. Chem.* **2004**, *14*, 2486–2488.
(37) Henderson, P.A.; Imrie, C.T. *Liq. Cryst.* **2005**, *32*, 673–682.
(38) Marcelis, A.T.M.; Giesbers, M.; Koudijs, A. *Liq. Cryst.* **2007**, *34*, 811–817.
(39) Imrie, C.T.; Stewart, D.; Remy, C.; Christie, D.W.; Hamley, I.W.; Harding, R.J. *Mater. Chem.* **1999**, *9*, 2321–2325.
(40) Wang, H.; Bai, B.; Zhang, P.; Long, B.; Tian, W.; Li, M. *Liq. Cryst.* **2006**, *33*, 445–450.
(41) Watanabe, J.; Komura, H.; Niori, T. *Liq. Cryst.* **1993**, *13*, 455–465.
(42) Watanabe, J.; Izumi, T.; Niori, T.; Zennyoji, M.; Takezoe, H. *Molec. Cryst. Liq. Cryst.* **2000**, *346*, 77–86.
(43) Weissflog, W.; Lischka, C.; Diele, S.; Wirth, I.; Pelzl, G. *Liq. Cryst.* **2000**, *27*, 43–50.
(44) Sepelj, M.; Lesac, A.; Baumeister, U.; Diele, S.; Nguyen, H.L.; Bruce, D.W.J. *Mater. Chem.* **2007**, *27*, 1154–1165.
(45) Blatch, A.E.; Luckhurst, G.R. *J. Mater. Chem.* **2000**, *27*, 775–787.
(46) Gray, G.W. In *The Molecular Physics of Liquid Crystals*; Luckhurst, G.R.; Gray, G.W., Eds; Academic Press: London, 1979; Chapter 1.
(47) Date, R.W.; Imrie, C.T.; Luckhurst, G.R.; Seddon, J.M. *Liq. Cryst.* **1992**, *12*, 203–238.

(48) Henderson, P.A.; Niemeyer, O.; Imrie, C.T. *Liq. Cryst.* **2001**, *28*, 463–472.
(49) Henderson, P.A.; Seddon, J.M.; Imrie, C.T. *Liq. Cryst.* **2005**, *32*, 1499–1513.
(50) Henderson, P.A.; Cook, A.G.; Imrie, C.T. *Liq. Cryst*. **2004**, *31*, 1427–1434.
(51) Emsley, J.W.; Luckhurst, G.R.; Shilstone, G.N.; Sage, I. *Mol. Cryst. Liq. Cryst. Lett.* **1984**, *102*, 223–233.
(52) Blatch, A.E.; Fletcher, I.D.; Luckhurst, G.R. *J. Mater. Chem.* **1997**, *7*, 9–17.
(53) Imrie, C.T. *Liq. Cryst.* **1989**, *6*, 391–396.
(54) Attard, G.S.; Imrie, C.T. *Liq. Cryst.* **1992**, *11*, 785–789.
(55) Attard, G.S.; Imrie, C.T.; Karasz, F.E. *Chem. Mater.* **1992**, *4*, 1246–1253.
(56) Blatch, A.E.; Fletcher, I.D.; Luckhurst, G.R. *Liq. Cryst*. **1995**, *18*, 801–809.
(57) McMillan, W.L. *Phys. Rev. A.* **1971**, *4*, 1238–1246.